Paper 05F-39

Modeling Benzene and Naphthalene Formation in a Premixed Propylene Flame

Hongzhi R. Zhang, Eric G. Eddings, Adel F. Sarofim
Department of Chemical Engineering
the University of Utah
Salt Lake City, UT 84112, USA
Corresponding Author: Hongzhi@crsim.utah.edu

Modeling Benzene and Naphthalene Formation in a Premixed Propylene Flame

Hongzhi R. Zhang*, Eric G. Eddings, Adel F. Sarofim
Department of Chemical Engineering, the University of Utah
Salt Lake City, UT 84112, USA

Abstract

The Utah Surrogate Mechanism was used to model a fuel-rich, non-sooting premixed laminar flame of propylene at 5000 Pa with an equivalence ratio of 2.32. The simulation results were found to be satisfactory in comparison with the experimental data. For example, the measured concentration profiles of the fuel, oxidizer, inert and major products were successfully reproduced. The predictive ability of the model for soot precursors is one of the major foci of this paper; the maximum acetylene and benzene concentrations were predicted within 15% and 30% of the measured values, respectively. The formation of benzene and naphthalene has been critically examined to identify the major reaction pathways of these smallest aromatics, the chemistry of which initiates the growth of PAH species. Combination reactions involving resonant stabilized species such as propargyl, allyl and benzyl radicals were found to be the most important formation pathways for aromatics. Reactions involving benzene have profound impacts on those of naphthalene; however, other formation routes bypassing benzene via reactions of C_3+C_4 were identified to be the major formation pathways of the higher aromatic species.

Introduction

The present paper is motivated by the need to develop and validate mechanisms that can be used to model the combustion phenomena of commercial fuels from natural gas to aviation fuel and the sooting behavior of these fuels. The focus of the paper therefore is on critical examination of the formation reaction pathways of aromatics in premixed flames in addition to the fuel consumption and major product formation routes. Olefin is one important class of species, and olefin concentration profiles are often measured in experiments. For example, Ingemarsson and coworkers (1999) measured the concentration profiles of six 1-alkene species (C_2-C_7) in their n-heptane oxidation experiment of a premixed laminar flame, and El Bakali et al. (1998) also reported concentration profiles of 1-alkenes in a rich laminar premixed n-heptane/O_2/N_2 flame (Φ=1.9). Later gas chromatography was used to identify structural isomers (El Bakali, 1999), even to distinguish the cis and trans configurations, that could not be distinguished in earlier experiments using mass spectrometry (El Bakali, 1998) and to provide added insights in how olefins are formed and consumed. The experimental structures of olefin species have aided the development of kinetic mechanisms that can be used to simulate

* Corresponding author, hongzhi@crsim.utah.edu

the combustion systems involving olefins, some of which have been assembled, modified and extended to form what the Utah Surrogate Mechanism. Of the olefin species, propylene is of particular interest in soot formation research because major aromatic precursors of acetylene and propargyl radical are easily formed from the fuel consumption. The investigation of propylene importance in the combustion research, however, is inadequate, if not largely overlooked.

The reaction kinetics of propylene is gaining more attention within the combustion community and it has been studied both experimentally and numerically as summarized by Simmie (2003). For example, a propylene model with 262 species and 1295 reactions from automatic mechanism generation was tested with ignition delay time in a shock tube (Heyberger, 2002) and with experimental data obtained in a jet-stirred reactor (Heyberger, 2001). Recent studies of propylene combustion emphasized on low-pressure premixed flames (Table 1) and the formation pathways of benzene (Table 2). For example, a fuel-rich, non-sooting (Φ=2.32) premixed laminar propylene flame at 5000Pa was investigated by Atakan and coworkers (1998) using combined laser techniques and MBMS to aid the understanding of the flame features in the regime between the sooting and stoichiometric equivalence ratio that are difficult to be modeled. Later on, the same group (2003) experimented another premixed flame burning a mixture of acetylene and propylene (1:1) in search of the unique flame features of this blended fuel with those of a premixed flame burning an equivalent atomic composition of pentadiene. Chemical reaction kinetics was also assembled to model the structure of premixed propylene flames. Hoyermann et al. (2004) proposed a propylene mechanism that was validated with selected concentration profiles measured in the two abovementioned flames in addition to data of flame speeds obtained in a counter-flow flame and those of ignition delays in shock tube experiments. The reaction pathways of benzene were discussed in details and those involving naphthalene in these flames have not been discussed thoroughly. The naphthalene chemistry and its relation with the core gas phase reactions of small aromatic fragments is one of the major foci of the present paper, complementing the data available in the literature of flame structures and benzene formation.

Table 1 Experimental Results on Propylene Oxidation

Investigators	Apparatus	Exp. Conditions	Measurement
Thomas et al. (1996)	premixed flame	37.5 torr, Φ=0.229	species profile
Atakan et al. (1998)	premixed flame	P=5000Pa, Φ=2.32	two dozen species, including radicals.
Davis et al. (1999)	plug flow reactor	atmospheric, <1200K, τ=4-180ms, Φ=0.7, 1.0, 1.4 and pyrolysis	species profile
	counter-flow twin flame	atmospheric, Φ=0.7-1.7	flame speed
Qin et al. (2001)	shock tube	T=1270-1820K, P=95-470kPa, Φ=0.5-2.0	ignition delay
Atakan et al. (2003)	premixed flame	P=5000Pa, C_3H_6/C_2H_2 (1:1), Φ=2.16	Species profile

Table 2 Models for Propylene Oxidation

Investigators	No. of RXN	No. of Species	Systems Modeled	Comment
Thomas et al. (1996)	323	57	premixed flame	The flame structures including the concentrations of intermediates were reproduced.
Davis et al. (1999)	71	469	plug flow reactor, counter-flow twin flame	A high temperature mechanism of propylene described the species profiles in a PFR very well and the flame speed in counter-flow flames if Φ is less than 1.
Heyberger et al. (2001)	1295	262	static vessel	Experimental temperature was between 580 and 740K and the negative temperature coefficient was reproduced at 630K.
	(automatically generated)		jet-stirred reactor	Experimental temperature was from 900 to 1200K and the profiles of a dozen species were reproduced.
			shock tube	The measured ignition delays (Qin, 2001; Burcat, 1985) were matched.
Bohm et al. (2000)			premixed flame	The reaction pathways of benzene and PAH formation were identified.
Hoyermann et al. (2004)	569	96	premixed flame, counter-flow twin flame, shock tube	The measured profiles of selected species in a C_3H_6 flame (products, C_2H_2, C_2H_4, C_3H_4, C_4H_2, C_4H_4, C_6H_6 and CH_3, C_3H_3, C_4H_3, C4H5 radicals) and a C_2H_2/C_3H_6 flame (fuels, C_2H_4, C_3H_4, and CH_3, C_3H_3, C_4H_3, C_4H_5 radicals) were reproduced. So were the flame speeds in a counter-flow flame and the ignition delays in shock tube experiments.

The importance of propylene chemistry in the aromatic formation is enforced by the formation of the allyl radical via hydrogen abstraction reactions. Allylic radicals determine the concentrations of many important aromatic precursors such as propyne, butyne, butene isomers and most unsaturated species that contribute to major formation routes of benzene, naphthalene and probably other higher aromatics. Thus a weakness in the chemistry of propylene may result in incorrect kinetics of one- or two-ring aromatics, and make the model vulnerable to changes of experimental conditions.

In this study, the Utah Surrogate Mechanism (version MECOFU 3.0 Beta) consisting of 208 species and 1087 reactions, validated with 40 premixed flames of various fuels

and conditions emphasizing the first ring formation, was modified and extended to fit the structure of a premixed flame of propylene experimented at 5000Pa with an equivalence ratio of 2.32. The goal of the extension is to improve the predictive power of the mechanism in the concentration profiles of the two-ring aromatic species of naphthalene and indene. Major formation and consumption pathways will be critically examined.

Experimental Data and Reaction Model

The Utah Surrogate Mechanism was extended and validated with the laminar premixed flame structure of propylene at 5000Pa ($\Phi = 2.32$, Atakan 1998). The simulator used was CHEMKIN III (Kee, 2003) and the thermodynamics data of species were obtained from CHEMKIN thermodynamic database (Kee, 1993) or estimated by THERGAS (Muller, 1995) employing Benson's additivity theory. The transport properties of species were obtained from CHEMKIN transport database (Kee, 1986) or estimated from those of similar species.

Numerical Performance of the Utah Surrogate Mechanism

The predicted concentration profiles of the feed and products in the propylene flame are compared with experimental data in Figure 1. The predicted concentration profiles of C_3H_6 and O_2 match the experimental data very well and that of inert argon has also been well predicted. The predicted concentrations of major products also provide a satisfactory validation of the mechanism. The experimental measurements of carbon monoxide are well reproduced with high accuracy in terms of mole fraction, formation rate and position; the largest deviation of the predicted carbon monoxide concentration is at the end of the reaction zone within 15%. The trends of the concentration profiles of water vapor and hydrogen gas are also accurately reproduced. The predicted profiles of these two species, however, are shifted vertically with the concentrations of molecular hydrogen over-predicted and those of water vapor under-predicted. Without ruling out other possible experimental errors, the uncertainty in the transport properties of the molecular hydrogen may be the major reason for the numerical discrepancy.

The predicted concentration profiles of major soot precursors reproduce the experimental data very well (Figure 2). These soot precursors participate two competing classes of aromatic formation pathways. The first aromatic ring is formed via the addition of acetylene onto C_4 radicals, complementing other ring formation pathways, namely the combination of C_3 radicals. The acetylene is also proposed as the major particle growth species via hydrogen abstracted intermediate PAH radicals. The predicted maximum mole fractions of C_2H_2, C_3H_4 isomers (allene and propyne) and C_3H_5 isomers (1-, 2-, 3-propenyl radicals) are within 15% of the experimental data. Those of C_3H_3, C_4H_3 isomers (H_2CCCCH and $HCCHCCH$) and C_4H_5 isomers (CH_2CHCCH_2, $CH_2CHCHCH$ and CH_3CHCCH) are within 30, 50, and 75% of the measured values, respectively. The scale of the numerical accuracy corresponds to the availability of kinetic data of these species. The position of the peak mole fraction is also predicted accurately for each of the selected soot precursors with the largest deviation seen in C_3 radicals about 0.05cm downstream.

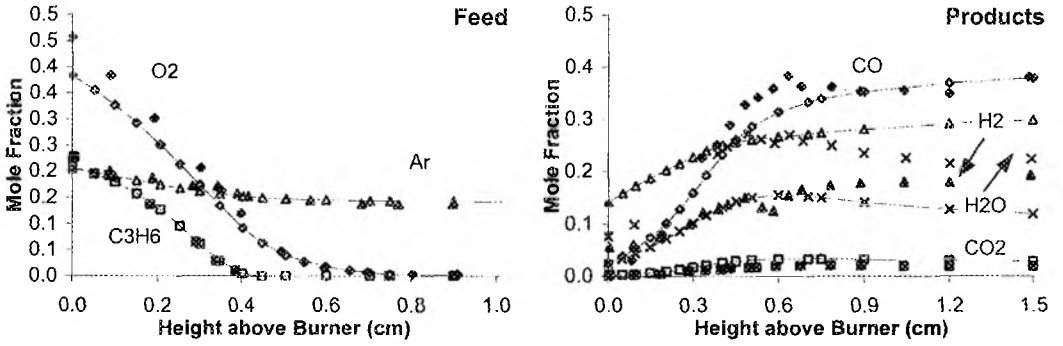

Figure 1. The predicted and the experimental concentration profiles of combustion feed (propylene, oxygen and argon) and products (hydrogen, water vapor, carbon oxides). The symbols represent the experimental data and the lines the simulations.

The extended mechanism over-predicts the maximum mole fraction of acetylene by 11.9% with the peak position matched. The net acetylene consumption rate surpasses the formation rate at locations upstream of 0.45cm above the burner surface, which is also the experimental and predicted position of the maximum concentration. The dominant formation reaction of acetylene is the dehydrogenation of vinyl radical and the selection of the rate was discussed in details somewhere else (Zhang, 2005). The addition reactions of acetylene onto singlet methylene and ethynyl radicals forming propargyl radical and diacetylene are two of the major consumption reactions of acetylene, complementing the oxidation of acetylene forming ethynyloxy radical (HCCO) and carbon monoxide. When the flame temperature is over 2200K at the post-flame zone, the importance of these reactions are displaced by that of the direct thermal decomposition of acetylene into ethynyl and hydrogen radicals. The thermal decomposition reaction rate used in the extended Utah Surrogate Mehcanism was proposed by Tsang (1986).

The measured and simulated concentration profiles of other important unsaturated intermediates are compared in Figure 3. The extended mechanism under-predicts the maximum mole fraction of ethylene by 32.2% but with the peak position of the profile matched. The under-prediction of the smallest but most abundant olefin, besides the fuel, may stem from many possible reasons, but notably the numerical discrepancy is lying on the lower boundary of the experimental uncertainty of 30% as reported by the Atakan and coworkers (1998). The predicted maximum mole fraction of C_4H_6 isomers is 29% higher than the measured value with the peak position of the profile predicted correctly. The three isomers (butyne CH_3CHCCH, 1,3-butadiene $CH_2CHCHCH_2$, 1,2-butadiene CH_3CHCCH_2) represent a roughly 10/40/50% distribution of the total concentrations of C_4H_6 species. The peak concentration of vinyl acetylene (CH_2CHCCH) is under-predicted by 7.7% only but the position of the profile is 0.07cm upstream compared to the experimental data. A larger numerical deviation of +72% is seen in the predicted maximum concentration of C_4H_8 isomers but with the peak position predicted correctly. 1-butene is the dominant isomer of 85% of the maximum concentration with the rest contributed from 2-butene and isobutylene.

Figure 3 also includes the comparisons between the predicted and measured concentrations of hydroxyl and methyl radicals. The predicted maximum concentration of

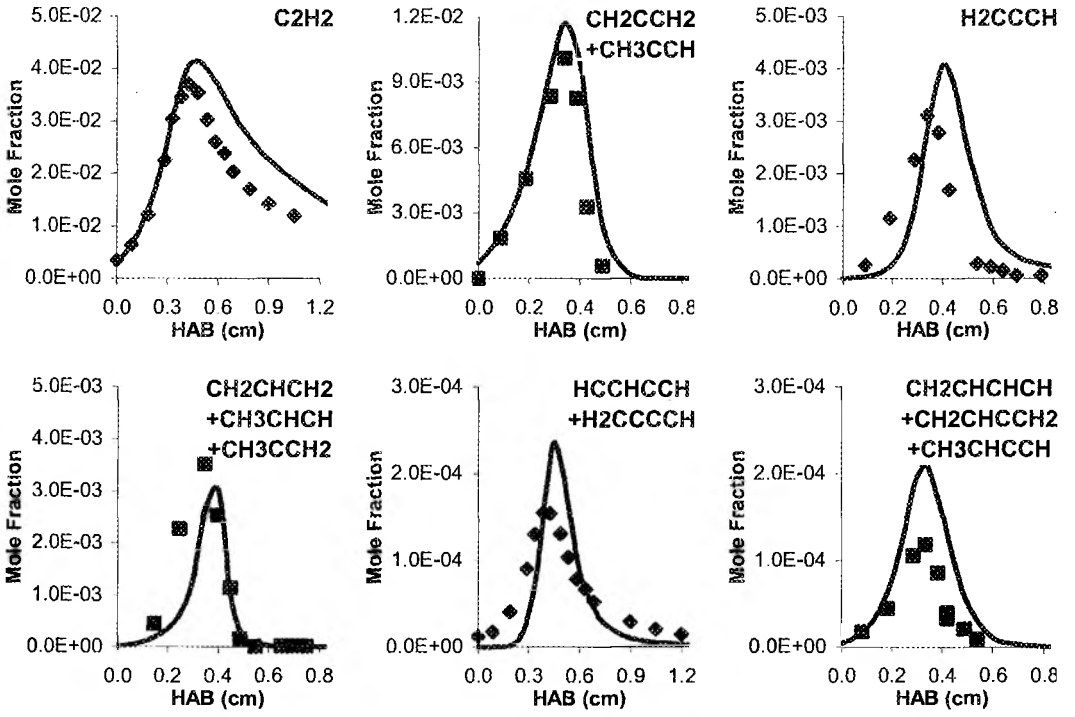

Figure 2. The predicted and the experimental concentration profiles of soot precursors (C_2H_2, C_3H_3 radical, C_3H_4, C_3H_5, C_4H_3 and C_4H_5 isomers). The symbols represent the experimental data and the lines the simulations.

hydroxyl radical is about one third of the measured value although the estimated peak position matches the experimental data. Critical examination is needed in the reactions involving the hydroxyl radical in order to understand the nature of the large discrepancy; on the other hand, the LIF techniques used to measure the OH concentration bear an experimental uncertainty of 50% reported by Atakan and coworkers. Also it is noteworthy that the Utah Surrogate Mechanism usually gives satisfactory predictions in the OH concentrations. For example, in most of the 14 flames, in which OH concentrations were measured (among the 40 validated premixed flames), the Utah Surrogate Mechanism gives sounded predictions of OH concentrations. These experiments include one methane, one methane ethane mixture, one natural gas (Turbiez, 2004), two acetylene (Westmoreland, 1986; Bastin, 1988), three ethylene (Peeters, 1973; Bhargava, 1998a, b), one propylene (Atakan, 1998), one butadiene (Cole, 1984), one benzene (Bittner, 1980) and three methanol flames (Vandooren, 1981), with a range of equivalence ratio from 0.21 to 2.32. The maximum concentration of OH radical was under-predicted in six of the fourteen flames and the numerical deviation was within 20% in four of the under-predicted flames (one methane, one ethylene, two methanol flames) and of -27.5% in the fifth flame (ethylene). More interestingly, besides the propylene flame studied in this paper, the predicted maximum concentration of OH radical is12% higher than the measured values averagely. Therefore, experimental uncertainties in the measurements of this species are also likely contributing to the numerical discrepancy.

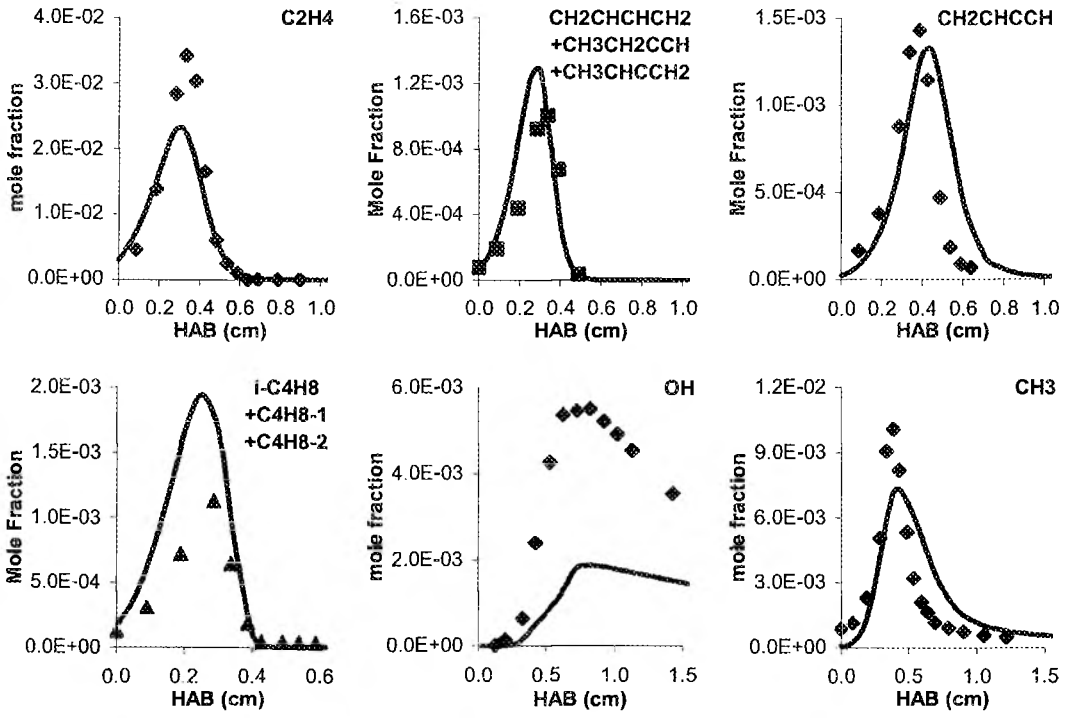

Figure 3. The predicted and the experimental concentration profiles of intermediate unsaturated species (ethylene, vinylacetylene, C_4H_6, and C_4H_8 isomers) and radicals (OH and CH_3). The symbols represent the experimental data and the lines the simulations.

The predicted maximum concentration of methyl radical is much better with a deviation of –27% only; the reported uncertainty in the measurements of this radical is a factor of three.

First Aromatic Rings Formation

The major formation pathways of benzene include the combination of C_3 species, namely those of H_2CCCH + H_2CCCH, H_2CCCH + CH_2CCH_2, and H2CCCH + CH_2CHCH_2. The acetylene additions onto C_4 radicals are of secondary importance in the benzene formation of the propylene flame studied in this paper even at lower temperature region (<1200K) where these reactions show significant contribution to the benzene formation in normal heptane flames. The propylene fuel of the flame can easily explain the dominance of the reactions involving C_3 species due to the preferential formation of these species as immediate products from the fuel decomposition (Figure 2). For example, the maximum concentrations of propargyl radical reported in the flames of acetylene (Westmoreland, 1986; Bastin, 1988) and benzene (Bittner, 1980) were around one thousandth of the reaction mixture, compared to three thousandth in this propylene flame; the maximum concentrations of 3-propenyl (allyl) radical were predicted of 100-

200PPM of the reaction mixtures in flames of normal heptane (El Bakali, 1999) and decane (Doute 1995), compared to 4000PPM measured in the propylene flame. The measured concentrations of C_3H_4 isomers offer another convincing example of the preferential formation of C_3 species as the maximum concentrations of these isomers account for 1% of the mixture, a factor of ten higher than those in most premixed flames (Zhang, 2005). The details of the benzene formation pathways have been discussed somewhere else (Zhang, 2005; Bohm, 2000).

The major formation pathways of naphthalene include five reaction classes: 1) the combination of cyclopentadienyl radicals; 2) the acetylene addition to benzene derivatives (HACA); 3) the combination of propargyl and benzyl radicals, similar to the combination of C_3 species for the benzene formation; and 4) Diels-Alder type reactions; 5) formation routes via naphthalene derivatives

Class 1:	$C_5H_5 + C_5H_5$	=	$C_{10}H_8 + H + H$
Class 2:	$C_6H_5CHCH + C_2H_2$	=	$C_{10}H_8 + H$
	$C_6H_4CHCH_2 + C_2H_2$	=	$C_{10}H_8 + H$
Class 3:	$C_6H_5CH_2 + H_2CCCH$	=	$C_{10}H_8 + H + H$
Class 4:	$C_6H_5 + CH_2CHCCH$	=	$C_{10}H_8 + H$
	$C_6H_5 + HCCHCCH$	=	$C_{10}H_8$
	$C_6H_5CCH + CH_2CH$	=	$C_{10}H_8 + H$
Class 5:	$C_{10}H_7 + H$	=	$C_{10}H_8$
	$C_{10}H_9$	=	$C_{10}H_8 + H$
	$C_{10}H_7CH_3 + H$	=	$C_{10}H_8 + CH_3$

The self-combination rate of the cyclopentadienyl radicals was taken from the LLNL butane mechanism (Marinov, 1998) with the energy barrier estimated at 8000cal. The rates of HACA reactions were taken from the similar reaction of C_2H_2 addition onto $CH_2CHCHCH$ in the Appel-Bockhorn-Frenklach (ABF) reaction mechanism (2000), since one of the authors proposed the original HACA concepts. The C_6H_5CHCH and $C_6H_4CHCH_2$ radicals are assumed chemically similar to the butadienyl radical considering that the aromatic ring contributes a 2π-electron system forming a dienyl radical moiety with the side chain. The rate of the propargyl addition in Reaction Class 3 proposed by Burcat and coworkers (1997) is in line with the rate used in the Ranzi mechanism (2000) at temperatures near 1000K and gradually approaches the upper limit of this reaction defined by Howard and coworkers (Richter, 2003). The Utah Surrogate Mechanism includes no analogous reactions of the other C_3 combination reactions ($H_2CCCH + CH_2CCH_2$ and $H_2CCCH + H_2CCCH$), which were identified as the major benzene formation pathways, since analogous reactions require a short-lived benzyne derivative species, the existence of which was only observed in specially designed experiments. The Reaction Class 4 includes naphthalene formation pathways similar to Diels-Alder type reactions of vinyl radical with vinyl acetylene or its radical HCCHCCH. The aromatic ring of the phenyl radical offers a vinyl moiety thus the reactions of $C_6H_5 + CH_2CHCCH$ and $C_6H_5CCH + CH_2CH$ were assigned the same rate proposed by Lindstedt and Skevis (1997) for the reference reaction $C_2H_3 + CH2CHCCH$. Howard (Richter, 2003), Ristori (2001) and coworkers also used the same rate for the reference reaction in their mechanisms and a similar rate for the reaction $C_6H_5 + CH_2CHCCH$ is

selected in the ABF mechanism, especially at temperatures higher than 1200K. The addition reaction rate of C_6H_5 + HCCHCCH used in the mechanism was proposed by Duran and coworkers (1988) for the similar reaction of C2H3 + HCCHCCH = C6H6 and the rate was adopted by Ristori (2001) for the reference reaction in their PAH mechanism. It is noteworthy that the rate is one order of magnitude higher than that used in the Howard mechanism (Richter, 2003) for the analogous reaction and that in the Milan mechanism for the reference reaction. The difference in the selected rates, however, will not dominate the predictions of naphthalene concentrations because the reaction is found of secondary importance via the reaction pathway analysis. The reactions involving $C_{10}H_7$ radical in Class 5 include a HACA-type addition of $C_6H_4CCH + C_2H_2 = C_{10}H_7$ using the same rate of the reference rate of HCCHCCH + C_2H_2 proposed by Frenklach and coworkers (Appel, 2000). The reaction, however, proceeds in the reverse direction of naphthyl decomposition.

The consumption of naphthalene includes the hydrogen abstraction by H and OH radicals and oxidation to naphthoxy radical.

Hydrogen Abstraction:	$C_{10}H_8 + H$	=	$C_{10}H_7 + H_2$
	$C_{10}H_8 + OH$	=	$C_{10}H_7 + H_2O$
Oxidation:	$C_{10}H_8 + O$	=	$C_{10}H_7O + H$

The major formation and consumption pathways of benzene and naphthalene have been compared in Figure 4. Benzene is formed from the self-combination of the propargyl radicals, the hydrogenation of the phenyl radical, and the transformation of fulvene; the rates of these reactions reach their maxima near 1700K. All three classes of major formation pathways have almost same importance in the first aromatic ring formation. Reactions involving the combination of other C_3 species also contribute to the formation of fulvene ($H_2CCCH + CH_2CHCH_2$ = FULVENE + H + H) and phenyl radical ($H_2CCCH + H_2CCCH = C_6H_5 + H$). Benzene is also formed via a minor C_3 species combination of the propargyl addition onto allene. The acetylene additions to the C_4 species are of secondary importance in the propylene flame in this study due to the preferential formation of C_3 species discussed earlier. The hydrogen abstraction by the H radical is the fastest consumption pathway of benzene near 1830K, at which the reaction reaches the maximum rate. The abstraction by H radical is nearly one order of magnitude faster than that by OH radical, a minor benzene consumption reaction that reaches the maximum rate near 1750K. The most important consumption pathway at higher temperature, however, reaches its peak rate around 2060K via thermal decomposition of benzene. The reaction involving the rupture of C-C bond ($C_6H_6 = H_2CCCH + H_2CCCH$) is twice faster than that involving the dehydrogenation ($C_6H_6 = C_6H_5 + H$). A similar scenario of dehydrogenation has been discussed earlier for the acetylene consumption, the maximum decomposition rate of which is found near 2200K since the *sp* hybridization of the carbon triple bond results in a stronger electron-withdrawing effect on the C-H sigma bond (more electronegative carbon) than the sp^2 hybridization of aromatic carbons.

The reactions involving naphthalene are simpler than those of benzene as seen in the Figure 4. For example, there is no analogous combination reaction of propargyl radicals since the possible reactants of benzene derivative are limited by electron valence. Neither

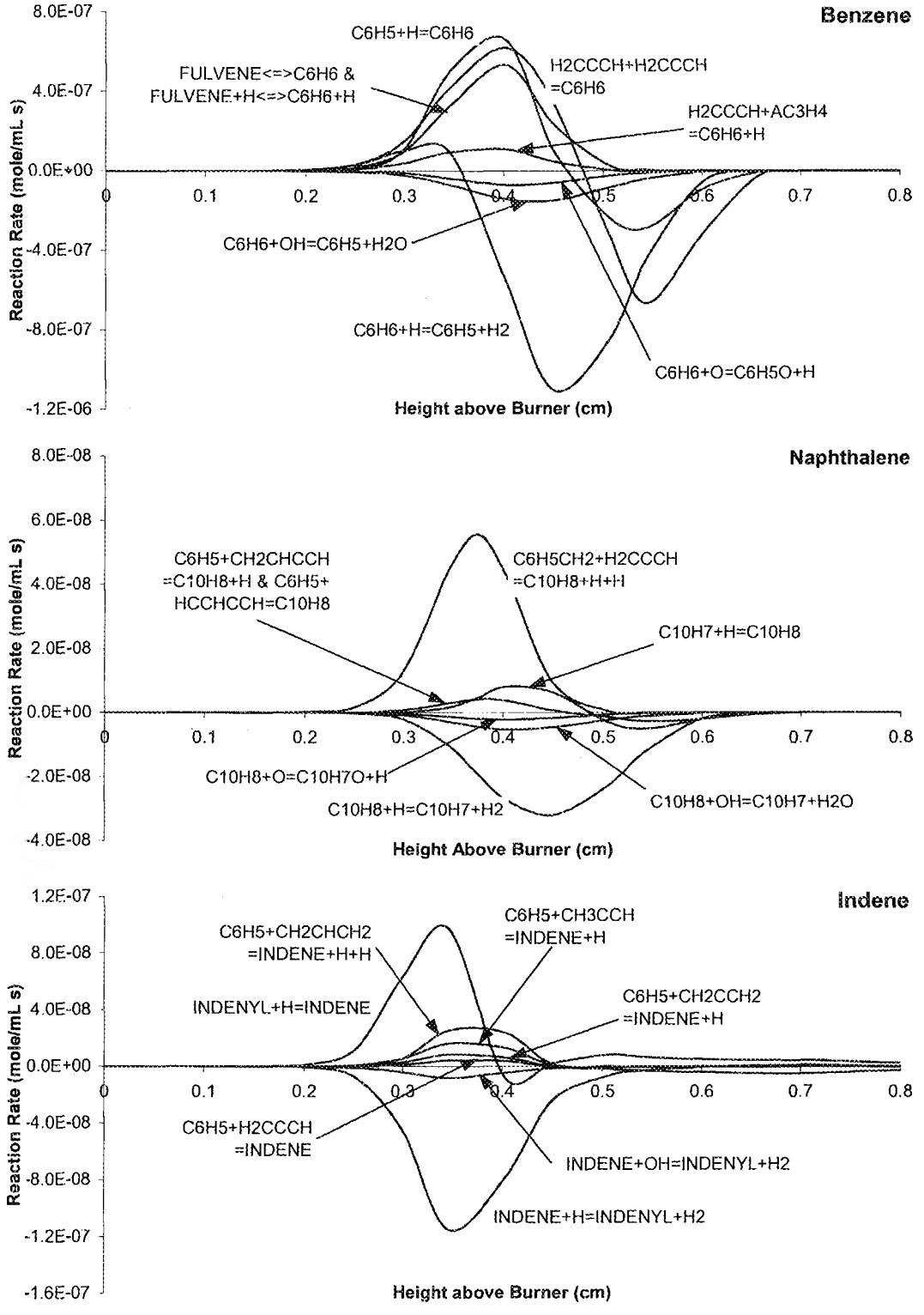

Figure 4. Formation and consumption reactions of benzene, naphthalene and indene using the extended Utah Surrogate Mechanism.

is the addition of the propargyl radical to allene. Naphthalene is formed mainly from the addition of the propargyl to the benzyl radical, the analogous reaction of which in the benzene formation is $H_2CCCH + CH_2CHCH_2$. The Diels-Alder type addition of phenyl radical to C_4 species contribute moderately toward the naphthalene formation. The abstraction reactions by the H and OH radicals dominate the naphthalene consumption and these reactions reach their maximum rates around 1850K with the H radical as the most powerful abstractor. Naphthalene is also consumed via the minor route of oxidation to naphthoxy radical, followed by the formation of indenyl radical.

The formation and consumption reactions of indene have been studied recently using the transition state theory of ab initio computational chemistry (Vereecken 2002, 2003). The proposed combination reactions of phenyl radical with allene and propyne have been included in the extended mechanism. Those reactions were found to be the major indene formation routes and their rates are only dwarfed by the combination rate of phenyl and allyl radicals. The rate of $C_6H_5 + CH_2CHCH_2$ was estimated with a pre-factor of 1.00×10^{13}, same as what used by Ristori and coworkers (2001) in a similar reaction of $C_2H_3 + CH_2CHCH_2$; the energy barrier was assigned a value of 3000 cal after the similar ring closure reaction of $H_2CCCH + CH_2CHCH_2$ (Burcat, 1997). The set of combination reactions of phenyl radical and C_3 species also includes that of propargyl radical ($C_6H_5 + H_2CCCH$), the rate of which has been proposed in Ranzi mechanism (2000). There are very few data of this reaction found in the literature and the reaction contributes moderately towards the indene formation. The combination of benzyl radical and acetylene ($C_6H_5CH_2 + C_2H_2$) was also proposed to be a potentially plausible formation route of indene in Vereecken computational chemistry study (2003) and the reaction or the similar reaction of $CH_2CHCH_2 + C_2H_2 = C_5H_6 + H$ has been included in the Howard (Richter, 2003), Ranzi (2000) and LLNL butane mechanisms (Marinov, 1998). The reaction involving C_6H_5 in the Howard mechanism and both reactions in the LLNL mechanism, however, used rates close to the high-pressure limit proposed by Vereecken and coworkers. Therefore in the extended mechanism the low-pressure rate that good for up to 10 atms was selected. It is noteworthy that the reverse reaction is preferred and the reaction is a major decomposition route of indene if the high-pressure rate is used; in the extended mechanism, however, the reaction is trivial compared to those of phenyl radical plus C_3 species. Another important indene formation pathway is the hydrogenation of indenyl radical, which is formed mainly from, besides the indene, the naphthoxy radical with the ejection of the molecular carbon monoxide, a reaction similar to the more studied reaction of C_6H_5O, probably due to its role in the naphthalene formation. It is very likely that indenyl radical is formed also from the combination of smaller fragments similar to those in the formation of indene. Those potential formation routes of indenyl radical, however, are not included in the current model due to the paucity of the literature. The major consumption reactions of indene are similar to those of benzene and naphthalene via the hydrogen abstraction by H and OH radicals with the H radical as the most powerful abstractor.

The missing combination reactions to indenyl radical are probably the major reason for the under-prediction of the maximum indene concentration of 61.9% as shown in Figure 5. The predicted maximum indene concentration, however, lies within the lower boundary of the experimental error, which was reported to be a factor of 3. Also substituted benzene ($C_6H_5CHCCH_2$ and $C_6H_5CH_2CCH$) were believed to be the major

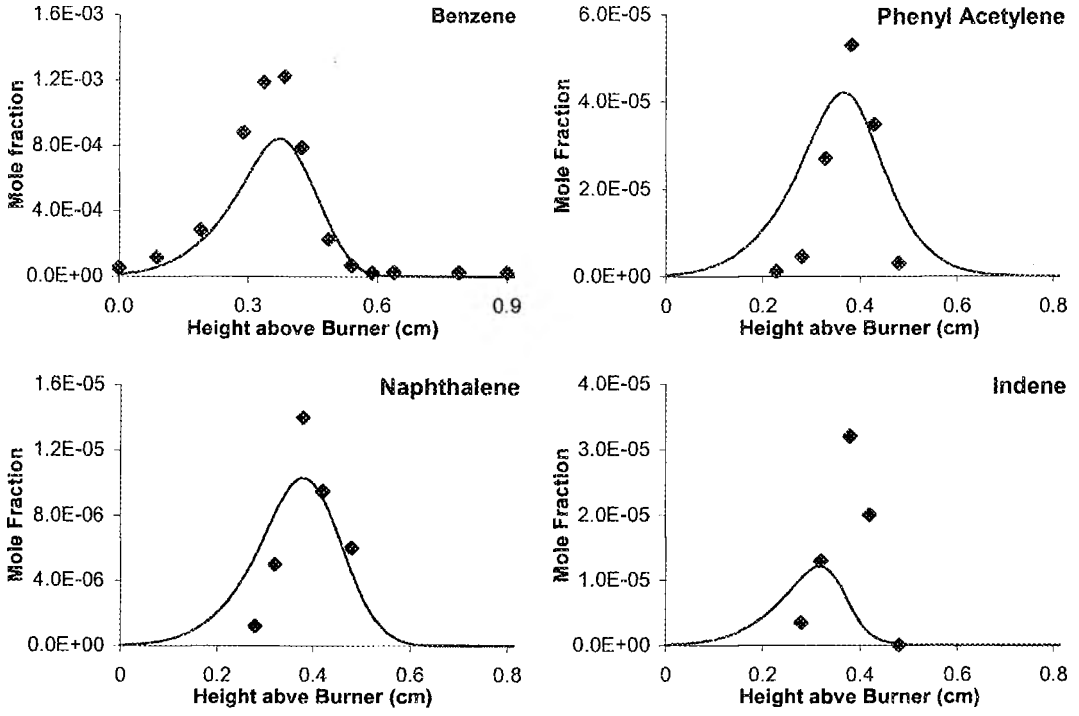

Figure 5. The predicted and the experimental concentration profiles of aromatics species (benzene, phenyl acetylene, naphthalene and indene). The symbols represent the experimental data and the lines the simulations. The measured concentration profiles of phenyl acetylene, naphthalene and indene have been shifted upstream by 0.1cm.

isomers of the measured concentration of C_9H_8 reported in earlier studies (Lindstedt, 2001; $C_6H_5CHCCH_2/C_6H_5CH_2CCH/INDENE \approx 2/2/1$), which is also a possible reason for the indene under-prediction since the other isomers are not included in the extended mechanism. The predicted maximum benzene concentration is 31.0% lower than the measured value with a reported uncertainty of 30%. That of phenyl acetylene is under-predicted of 21.6% and the experimental uncertainty of this species was reported to be a factor of three. The uncertainty of the measured naphthalene concentrations was also reported around 30% and the extended Utah Surrogate Mechanism is able to predict the maximum with a discrepancy of -26.4%. The predicted positions of the peak concentration of four aromatic species are also inline with the measurements after the profiles of phenyl acetylene, naphthalene and indene have been shifted upstream by 0.1cm. The shift was guided by the position of benzene profile since the phenyl acetylene and benzene are expected to have similar flame structures.

Conclusion

The competing benzene formation pathways via combinations of resonantly stabilized C_3 species ($H_2CCCH + H_2CCCH$, $H_2CCCH + CH_2CCH_2$, and $CH_2CHCH_2 + H_2CCCH$),

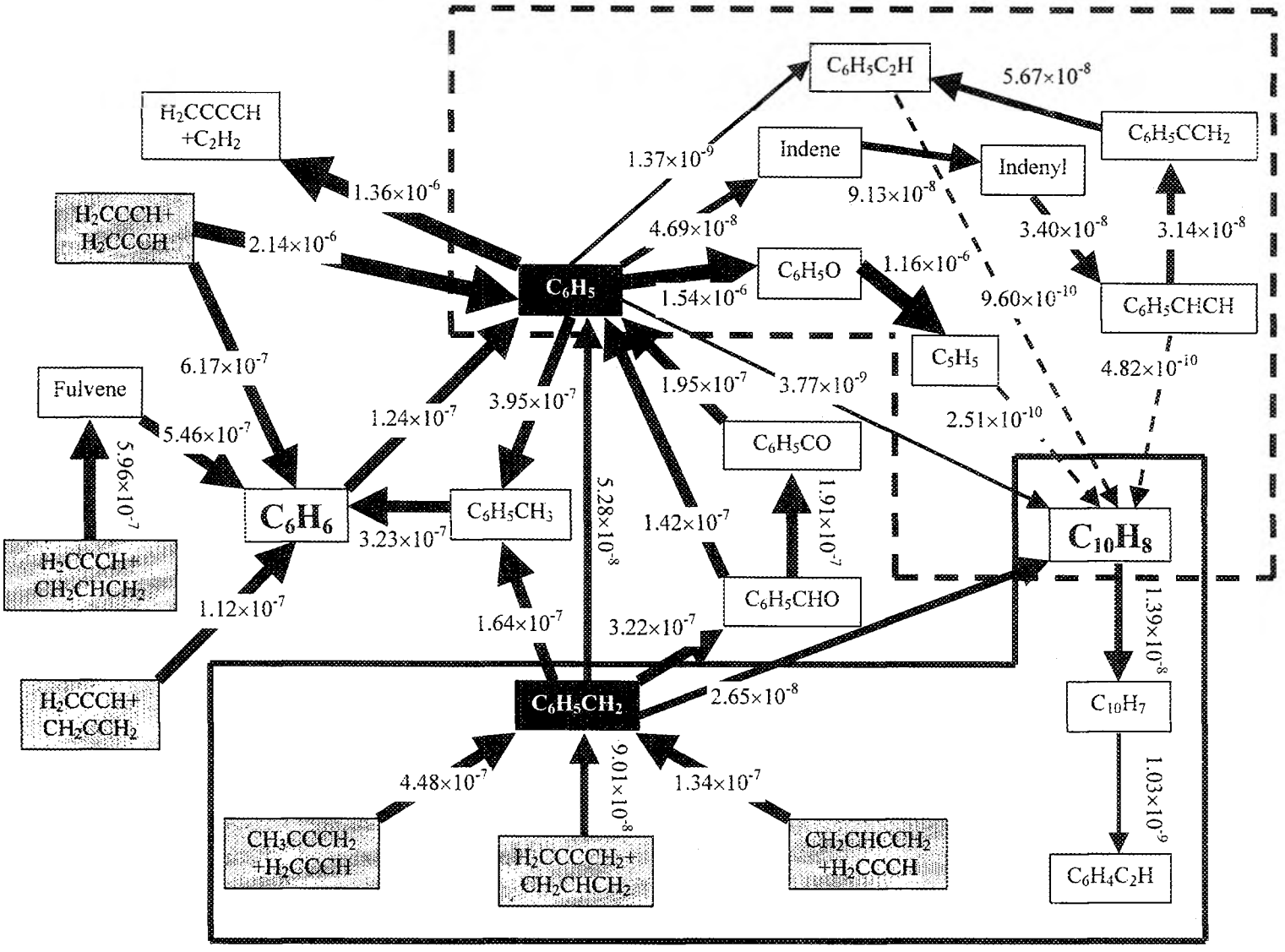

Figure 6 Major formation and consumption pathways of benzene, naphthalene and indene.

and the acetylene addition onto C_4 radicals (C_2H_2 + HCCHCCH and C_2H_2 + $CH_2CHCHCH$) are the most studied reactions within the combustion simulation community. So are the pathways of naphthalene formation via the combination of the resonantly stabilized cyclopentadienyl radicals ($C_5H_5 + C_5H_5 = C_{10}H_8 + H + H$), the acetylene addition ($C_6H_5CHCH + C_2H_2$, $C_6H_4C_2H + C_2H_2$ and $C_6H_4CHCH_2 + C_2H_2$). The less known naphthalene pathways include the combination of the resonantly stabilized benzyl and propargyl radicals ($C_6H_5CH_2 + H_2CCCH$) and the addition of vinyl moieties onto highly unsaturated C_4 moieties (C_6H_5 + CH_2CHCCH, C_6H_5 + HCCHCCH and $C_6H_5CCH + CH_2CH$). After the good agreements between the predicted and measured concentrations of benzene, naphthalene and indene were obtained, the major formation and consumption pathways of these aromatic species were identified. In Figure 6, the rates of most important pathways involving major aromatic species are shown along the arrow indicating the reaction direction and the thickness of the arrow represents the magnitude of reaction rate in orders.

The combinations of C_3 species are identified to be the major formation pathways of benzene in Figure 6 in addition to other competing reactions. Benzene is formed directly from C_3 species or via the intermediates of fulvene and phenyl radical. The acetylene addition reactions make minor contribution to the benzene formation. The precursors of the benzene formation from smaller hydrocarbon fragments are presented with the filled boxes. Abundant literature sources of benzene formation have been generated; therefore the aromatic formation reactions to be discussed here are those of naphthalene.

The major formation reaction classes of naphthalene proposed in earlier studies have been included in Figure 6. For example, the combination of resonantly stabilized cyclopentadienyl radicals was found to be an inadequate formation route of naphthalene, the rate of which is two orders of magnitude lower than the fastest formation route via the combination of benzyl and propargyl radicals. The Utah Surrogate Mechanism was tested in quite a few premixed flames for the numerical accuracy in prediction of the concentrations of cyclopentadienyl radical and its parent molecule. In the Bittner benzene flame (1980) the maximum concentration of the radical was over-predicted by 83.7%. In eight other flames, in which the concentrations of cyclopentadiene were measured, good agreements were obtained for the two benzene flames (Bittner, 1980; Tregrossi, 1999) and the predicted concentrations were inline with the methane and the ethane flames (Marinov, 1996). The maximum concentration of cyclopentadiene was over-predicted of a factor of 2.4 in a propane flame (Marinov, 1997) and under-predicted of a factor of 6.9 in another propane flame (Cool, 2005). More interestingly, those in two olefin (ethylene) flames were under-predicted by a factor of 5 (Castaldi, 1996) and 30 (Tregrossi, 1999). Therefore, the possibly under-predicted concentration of cyclopentadienyl radical may result in the slower formation of naphthalene. Besides the combination of C_5 radicals, the acetylene additions onto $C_6H_5C_2H$, C_6H_5CHCH and $C_6H_4C_2H$ are also negligible as indicated by the dashed arrows. Furthermore, the reaction of $C_6H_4C_2H + C_2H_2$ is a consumption route of naphthalene rather than contributing to its formation. Those two minor formation reaction classes are summarized in the box with dashed border.

The major formation routes of naphthalene are Diels-Alder reactions of vinyl and C_4 moieties and the combination of benzyl and propargyl radicals that have been discussed in earlier sections; the reaction involving benzyl radical is one order of magnitude higher than the Diels-Alder reactions. The major consumption reaction of benzyl radical,

however, is the oxidation of the side chain radical site to benzaldehyde (C_6H_5CHO), which in turn decomposes to phenyl radical via the ejection of the side chain functional group. The hydrogenation of the benzyl radical is another major consumption pathway. Both consumption reactions are one order of magnitude faster than the combination with propargyl radical leading to naphthalene. On the other hand, the major formation routes of benzyl radical do not involve the one-ring aromatic species of benzene and it radical. The benzyl radical is formed from the combinations of C_3 and C_4 species ($CH_3CCCH_2 + H_2CCCH = C_6H_5CH_2 + H$, $H_2CCCCH_2 + CH_2CHCH_2 = C_6H_5CH_2 + H + H$ and $CH_2CHCCH_2 + H_2CCCH = C_6H_5CH_2 + H$) and these reactions are adequate to model its formation. For example, the maximum concentration of benzyl radical was over-predicted by a factor of 6.8 in a butadiene flame (Cole, 1984) and under-predicted by 30% in a benzene flame (Bittner, 1980); the concentrations of benzyl radical were measured in only two of the forty premixed flames validated using the Utah Surrogate Mechanism. Although other combination reactions are also potential, plausible routes for benzyl radical, the mechanism only includes these three due to the paucity of the literature for reaction rates.

One important discovery from the identification of the major reaction routes of naphthalene is the parallel formation of the first aromatic species of benzene and naphthalene. Benzene and naphthalene are formed from the combination of smaller hydrocarbon fragments that competing with each other for C_3 and C_4 species rather than the gradual buildup via the molecular addition of small species, the rate of which is dwarfed by one order of magnitude. It is also noteworthy that the growth route from benzene to benzyl radical to naphthalene is blocked at the link of intermediate as a result of the extra stability of the benzyl radical due to the resonant structures; the reaction between the benzyl radical and its parent molecule favors the toluene formation. The major reaction pathways of naphthalene formation that are parallel to and competing with those of benzene are included in the box with straight-line borders.

The parallel formation of the smallest aromatic species has important impacts on the development of soot formation models since very often only one aromatic species is selected to be the nucleation seed and growth precursors in these models (Appel, 2000; Zhang, 2003; Dobbins, 1997). The independent, parallel formation routes of small aromatic species make the inclusion of multiple precursors of different sizes a plausible, more realistic approach in the PAH and soot formation models.

References

Appel, J., Bockhorn, H., Frenklach, M. (2000) Kinetic modeling of soot formation with detailed chemistry and physics: laminar premixed flames of C2 hydrocarbons. *Combustion and Flame*, **121**(1/2), 122.

Atakan, B., Hartlieb, A.T., Brand, J., Kohse-Hoinghaus, K. (1998) An experimental investigation of premixed fuel-rich low-pressure propene/oxygen/argon flames by laser spectroscopy and molecular-beam mass spectrometry. *Proc. Combust. Inst.*, **27**:435-444.

Atakan, B., Lamprecht, A., Kohse-Hoinghaus, K. (2003) An experimental study of fuel-rich 1,3-pentadiene and acetylene/propene flames. *Combustion and Flame*, **133**(4), 431-440.

Bastin, E., Delfau, J. L., Reuillon, M., Vovelle, C., Warnatz, J. (1989) Experimental and computational investigation of the structure of a sooting acetylene-oxygen-argon flame. *Symposium (International) on Combustion*, **22**, 313.

Bhargava, A., and Westmoreland, P. R. (1998a) Measured flame structure and kinetics in a fuel-rich ethylene flame, *Combustion and Flame*, **113**, 333.

Bhargava, A., and P. R. Westmoreland (1998b) MBMS analysis of a fuel-lean ethylene flame, *Combustion and Flame*, **115**, 456.

Bittner, J. D., and Howard, J. B. (1980) Composition profiles and reaction mechanisms in a near-sooting premixed benzene/oxygen/argon flame. *Symposium (International) on Combustion*, **18**, 1105.

Bohm, H., Lamprecht, A., Atakan, B., Kohse-Hoinghaus, K. (2000) Modelling of a fuel-rich premixed propene-oxygen-argon flame and comparison with experiments. *Physical Chemistry Chemical Physics*, **2**(21), 4956-4961.

Burcat, A., Radhakrishnan, K. (1985) High-temperature oxidation of propene. *Combustion and Flame*, **60**(2), 157-69.

Burcat, A. and Dvinyaninov, M. (1997) Detailed kinetics of cyclopentadiene decomposition studied in a shock tube, *Int. J. Chem. Kinet.*, **29**, 505.

Castaldi, M. J., Marinov, N. M., Melius, C. F., Huang, J., Senkan, S. M., Pitz, W. J. and Westbrook, C. K. (1996) Experimental and modeling investigation of aromatic and polycyclic aromatic hydrocarbon formation in a premixed ethylene flame. *Symposium (International) on Combustion*, **26** (Vol. 1), 693.

Cool, T. A., Nakajima, K., Taatjes, C. A., McIlroy, A., Westmoreland, P. R., Law, M. E., Morel, A. (2005) *Proceedings of the Combustion Institute*, **30**, 1681.

Cole, J. A., Bittner, J. D., Longwell, J. P., and Howard, J. B. (1984) Formation mechanisms of aromatic compounds in aliphatic flames. *Combustion and Flame*, **56**(1), 51.

Davis, S. G., Law, C. K. and Wang, H. (1999) Propene pyrolysis and oxidation kinetics in a flow reactor and laminar flames. *Combustion and Flame*, **119(4)**, 375.

Dobbins, R. A. (1997) The early soot particle formation in hydrocarbon flames. Combustion Science and Technology Book Series, **4** (Physical and Chemical Aspects of Combustion), 107.

Doute, C.; Delfau, J. L.; Akrich, R.; Vovelle, C. (1995) Chemical structure of atmospheric pressure premixed n-decane and kerosene flames. *Combustion Science and Technology*, **106**, 327.

Duran, R. P., Amorebieta, V. T., and Colussi, A. J. (1988) Is the homogeneous thermal dimerization of acetylene a free-radical chain reaction? Kinetic and thermochemical analysis. *J. Phys. Chem.*, **92**, 636.

El Bakali, A., Delfau, J. L. and Vovelle, C. (1998) Experimental study of 1 atmosphere, rich, premixed n-heptane and iso-octane flames. *Combustion Science and Technology*, **140**, 69.

El Bakali, A., Delfau, J. L. and Vovelle, C. (1999) Kinetic modeling of a rich, atmospheric pressure, premixed n-heptane/O2/N2 flame. *Combustion and Flame*, **118**, 381.

Heyberger, B., Battin-Leclerc, F., Warth, V., Fournet, R., Come, G. M. and Scacchi, G. (2001) Comprehensive mechanism for the gas-phase oxidation of propene, *Combustion and Flame*, **126**, 1780.

Heyberger, B., Belmekki, N., Conraud, V., Glaude, P. A., Fournet, R. and Battin-Leclerc, F. (2002) Oxidation of small alkenes at high temperature, *International Journal of Kinetics*, **34**, 666.

Hoyermann, K., Mauss, F., Zeuch, T. (2004) A detailed chemical reaction mechanism for the oxidation of hydrocarbons and its application to the analysis of benzene formation in fuel-rich premixed laminar acetylene and propene flames. *Physical Chemistry Chemical Physics*, **6**(14), 3824-3835.

Ingemarsson, A. T., Pedersen, J. R. and Olsson, J. O. (1999) Oxidation of n-heptane in a premixed laminar flame. *Journal of Physical Chemistry A*, **103(41)**, 8222.

Kee, R. J., Dixon-Lewis, G., Warnatz, J., Coltrin, M. E. and Miller, J. A. (1986) The Chemkin transport database. *Sandia Report #SAND 86-8246.*

Kee, R. J., Rupley, F. M. and Miller, J. A. (1993) The Chemkin thermodynamic database. *Sandia Report #SAND 87-8215B.*

Kee, R. J., Rupley, F. M., Miller, J. A., Coltrin, M. E., Grcar, J. F., Meeks, E., Moffat, H. K., Lutz, A. E., Dixon-Lewis, G., Smooke, M. D., Warnatz, J., Evans, G. H., Larson, R. S., Mitchell, R. E., Petzold, L. R., Reynolds, W. C., Caracotsios, M., Stewart, W. E., Glarborg, P., Wang, C., Adigun, O., Houf, W. G., Chou, C. P. and Miller, S. F. (2003) Chemkin Collection, Release 3.7.1, Reaction Design, Inc, San Diego, CA.

Lindstedt, R. P., Skevis, G. (1997) Chemistry of acetylene flames. *Combustion Science and Technology*, **125**(1-6), 73.

Lindstedt P., Maurice L., and Meyer M. (2001) Thermodynamic and kinetic issues in the formation and oxidation of aromatic species. *Faraday discussions*, 119, 409.

Marinov, N. M., Pitz, W. J., Westbrook, C. K., Castaldi, M. J. and Senkan, S. M. (1996) Modeling of aromatic and polycyclic aromatic hydrocarbon formation in premixed methane and ethane flames. *Combustion Science and Technology*, **116-117**, 211.

Marinov, N. M., Castaldi, M. J., Melius, C. F., and Tsang, W. (1997) Aromatic and polycyclic aromatic hydrocarbon formation in a premixed propane flame. *Combustion Science and Technology*, **128**(1-6), 295.

Marinov, N. M., Pitz, W. J., Westbrook, C. K., Vincitore, A. M., Castaldi, M. J., Senkan, S. M., Melius, C. F. (1998) Aromatic and polycyclic aromatic hydrocarbon formation in a laminar premixed n-butane flame. *Combustion and Flame*, **114**(1/2), 192.

Muller, C., Michel, V., Scacchi, G. and Côme, G. M. (1995) THERGAS: a computer program for the evaluation of thermochemical data of molecules and free radicals in the gas phase. *J. Chim. Phys.*, **92**, 1154.

Peeters, J., and G. Mahnen (1973) Proceedings of the First European Symposium on Combustion, Sheffield, England, 245.

Qin, Z., Yang, H., Gardiner, W. C., Jr. (2001) Measurement and modeling of shock-tube ignition delay for propene. *Combustion and Flame*, **124**(1/2), 246-254.

Ranzi, E., Dente, M., Goldaniga, A., Bozzano, G. and Faravelli, T. (2000) Lumping procedures in detailed kinetic modeling of gasification, pyrolysis, partial oxidation and combustion of hydrocarbon mixtures. *Progress in Energy and Combustion Science*, Volume Date 2001, **27(1)**, 99.

Richter, H., Granata, S., Green, W. H., Kronholm, D. F. and Howard, J. B. (2003) Detailed modeling of PAH and soot formation in flames. *Proceedings of the European Combustion Meeting.*

Ristori, A., Dagaut, P., El Bakali, A., Pengloan, G., Cathonnet, M. (2001) Benzene oxidation: experimental results in a JDR and comprehensive kinetic modeling in JSR, shock-tube and flame. *Combustion Science and Technology*, **167**, 223.

Simmie, J. M. (2003) Detailed chemical kinetic models for the combustion of hydrocarbon fuels. *Progress in Energy and Combustion Science*, **29(6)**, 599.

Thomas, S. D., Bhargava, A., Westmoreland, P. R., Lindstedt, R. P., Skevis, G. (1996) Propene oxidation chemistry in laminar premixed flames. *Bulletin des Societes Chimiques Belges*, **105**(9), 501-512.

Tregrossi, A., Ciajolo, A. and Barbella, R. (1999) The combustion of benzene in rich premixed flames at atmospheric pressure. *Combustion and Flame*, **117**, 553.

Tsang, W., Hampson, R. F. (1986) Chemical kinetic data base for combustion chemistry. Part I. Methane and related compounds. *J. Phys. Chem. Ref. Data*, **15**, 1087.

Turbiez, A., El Bakali, A., Pauwels, J. F., Rida, A., and Meunier, P. (2004) Experimental study of a low pressure stoichiometric premixed methane, methane-ethane, methane-ethane-propane and synthetic natural gas flames, *Fuel*, **83**, 933.

Vandooren, J. and van Tiggelen, P. J. (1981) Experimental Investigation of Methanol Oxidation in Flames; Mechanisms and Rate Constants of Elementary Steps, *Symposium (International) on Combustion*, **18**, 473.

Vereecken, L., Peeters, J., Bettinger, H. F., Kaiser, R. I., Schleyer, P. v. R. and Schaefer, H. F. (2002) Reaction of phenyl radicals with propyne. *J. AM. CHEM. SOC.*, **124**(11), 2781.

Vereecken, L. and Peeters, J. (2003) Reactions of chemically activated C9H9 species II: The reaction of phenyl radicals with allene and cyclopropene, and of benzyl radicals with acetylene. *Phys. Chem. Chem. Phys.*, **5**, 2807.

Westmoreland, P. R., Howard, J. B. and Longwell, J. P. (1986) Tests of published mechanisms by comparison with measured laminar flame structure in fuel-rich acetylene combustion. *Symposium (International) on Combustion*, **21**, 773.

Zhang, H. R., Violi, A., Sarofim, A. F. and Frenklach, M. (2003) A simulation of soot formation using particle dynamics with one dimensional nucleation", 3rd US Joint Meeting, The Combustion Institute, Chicago, Illinois, March 16-19th, 2003.

Zhang, H. (2005) Chapter 5, PhD dissertation, the Department of Chemical Engineering, the University of Utah, May, 2005.